Ionics (2019) 25:231–239
https://doi.org/10.1007/s11581-018-2591-6

ORIGINAL PAPER

1-Ethyl-2,3-dimethylimidazolium tetrafluoroborate ionic liquid mixture as electrolyte for high-voltage supercapacitors

Qingguo Zhang [1,2] · Huige Yang [2] · Xiaoshi Lang [1] · Xinyuan Zhang [2] · Ying Wei [2]

Received: 18 March 2018 / Revised: 28 April 2018 / Accepted: 5 May 2018 / Published online: 8 June 2018

Abstract

A novel ionic liquid (IL) 1-ethyl-2,3-dimethylimidazolium tetrafluoroborate ([Emmim][BF_4]) with trialkyl substitution imidazolium cation was synthesized, and its binary system blended with acetonitrile (ACN) under different concentrations were prepared and investigated as possible electrolytes for supercapacitors. The physico-chemical properties such as density, viscosity, and electrical conductivity of the binary mixture system were measured from 288.15 to 333.15 K. The temperature dependences of density, viscosity, and electrical conductivity were illustrated and discussed by the Vogel-Fulcher-Tamman (VFT) equation and Arrhenius equation. It was found that the VFT equation was more suitable to [Emmim][BF_4] + ACN system. Further, the important characteristics of this IL-based electrolyte for supercapacitors including the maximum operative voltage, the capacitance, the energy density, and power density were measured and calculated by cyclic voltammetry (CV), electrochemical impedance spectrum (EIS), and galvanostatic charge-discharge. The results show that the performance of the electrolyte can be improved with appropriate ratio of IL. When the concentration of the IL increased to 0.8 mol L^{-1}, the maximum operative voltage increased to 5.9 V, and the specific capacitance achieves 142.6 F g^{-1}. It shows the IL-based mixtures with excellent characteristics are applicable as high-voltage electrolytes for supercapacitors.

Keywords Ionic liquid · Electrolyte · Supercapacitor · Thermodynamic property · Electrochemical performance

Introduction

The electrochemical capacitors, also referred as supercapacitors, have been widely used in various fields with high power density and excellent life cycle [1–4]. There are two typical energy storage classifications of supercapacitors: electrical double layer capacitors (EDLC) and pseudocapacitors [5]. Recently, research on EDLCs has aroused great interest because of the rise in popularity of electric and hybrid electric vehicles. Carbon-based supercapacitors have attracted a lot of attention due to the diversified material structures of higher stability and conductivity [6–8]. The supercapacitors' superior properties benefit from their unique energy storage mechanism. The energy arises from the electrical charges' accumulation at the electrode/electrolyte interface to form the electrical double-layer through rapidly adsorption-desorption without faradic reactions [9–12]. However, the weakness for the supercapacitors is the low energy density. Many studies have been carried out to improve the energy density to meet the expanding demands. As is known, the energy density of supercapacitors can be described by the equation $E = ½CV^2$, where C is the capacitance, and V is the operative voltage of supercapacitors. It is evident that increasing the supercapacitors' operative voltage can have a great impact on the supplied energy. Generally, the operative voltage of a supercapacitor does not exceed 1.0 V in aqueous media due to the decomposition voltage of water, and for most of organic electrolytes, the safe operative voltages are generally lower than 2.7 V [13–15].

Ionic liquids (ILs) are room temperature molten salts with negligible vapor pressure, low flammability, wide electrochemical windows, and high electrochemical and

Electronic supplementary material The online version of this article (https://doi.org/10.1007/s11581-018-2591-6) contains supplementary material, which is available to authorized users.

✉ Qingguo Zhang
zhangqingguo@bhu.edu.cn

✉ Ying Wei
weiying2001_77@163.com

[1] College of New Energy, Bohai University, Jinzhou 121013, Liaoning Province, China

[2] College of Chemistry and Chemical Engineering, Bohai University, Jinzhou 121013, Liaoning Province, China

Table 1 Information of sample

Chemical name	Source	Initial mole faction purity	Purification method	Final mole fraction purity	Analysis method
Bromoethane	Sinopharm (China)	> 0.990	Distillation	0.997	GC[a]
Sodium tetrafluoroborate	Sinopharm (China)	0.995	Precipitation	> 0.995	
1, 2-dimethylimidazolium	Zhejiang doubleport (China)	> 0.990	Distilled at reduced pressure	> 0.998	^{1}HNMR
Acetonitrile	Sinopharm (China)	> 0.990	Distillation	> 0.997	GC, KF[b]

[a] Gas–liquid chromatography

[b] Karl Fischer titration

thermal stabilities [16–18]. Among the alternative electrolytes proposed so far, ILs can offer a wide range of electrochemical stability, which are currently considered as one of the most promising materials as high-performance electrolytes. Many studies showed that the operative voltage of IL-based supercapacitors can realize 3.5 V or even higher [16, 19–21].

However, the typically high viscosity and low conductivity of the ILs limit the powers of IL-based supercapacitors, especially at room temperature. In order to improve the power of high-voltage supercapacitors, the low viscosity mixtures resulted from a combination of ILs, organic solvents, or other liquids have been a useful and easy method [16, 21, 22]. Krause et al. have shown the mixtures of 1-butyl-1-methylpyrrolidinium bis{(trifluoromethyl)sulfonyl}imide ([Pyrr$_{14}$][TFSI]), and PC exhibits higher conductivity and lower viscosity at 298 K than those of the neat [Pyrr$_{14}$][TFSI], while still keeping an operative voltage as high as 3.5 V [23]. Christoph Schütter et al. have reported to the blends of nitriles (butyronitrile and adiponitrile) and [Pyrr$_{14}$][TFSI] in EDLCs revealed a good electrochemical stability allowing a maximum operative voltage up to 3.7 V [24]. Brandt et al. studied mixtures of the trimethylsulphoniumbis[(trifluoromethyl)sulphonyl]imide (Me_3STFSI) and PC as electrolyte for carbon-based electrochemical double layer capacitors (EDLC). They demonstrated that the EDLC life cycle strongly depends on the concentration of Me_3STFSI in the mixture [25].

Herein, we synthesized trialkyl substitution imidazolium-based IL [Emmim][BF_4] and characterized it by ^{1}H nuclear magnetic resonance spectroscopy (^{1}HNMR), infrared spectrum (IR), thermogravimetry (TGA), and elemental analysis (EA), respectively. For the solid state of [Emmim][BF_4], the ACN was used as solvent to prepare a series of IL binary mixture system (concentration of IL from 0.2 to 1.2 mol·L^{-1}). First, the density, viscosity, and electrical conductivity of the [Emmim][BF_4] + ACN binary system were measured at temperature range from 288.15 to 333.15 K. The temperature dependences on electrical conductivity of the binary system under different concentrations were described by the Vogel-Fulcher-Tamman (VFT) equation and Arrhenius equation, respectively. Then, the IL mixtures were employed as possible electrolytes in the active carbon-based supercapacitors. The cyclic voltammetry (CV), electrochemical impedance spectrum (EIS), and galvanostatic charge-discharge (GCD) of the supercapacitors were measured and discussed. In addition, the energy and the power of the investigated devices were calculated to evaluate the electrochemical performances of the fabricated supercapacitors. The results showed the [Emmim][BF_4] + ACN binary mixture electrolytes could be a good candidate of electrolyte with great potential for supercapacitors.

Experimental section

Chemicals

Bromoethane, sodium tetrafluoroborate, and acetonitrile are purchased from Sinopharm Co (China) (purity > 0.990). The 1,2-dimethylimidazolium is purchased from Zhejiang doubleport Co. Ltd. (China) and distilled at reduced pressure before use. The materials' purities and sources are summarized in Table 1.

Synthesis

The IL 1-ethyl-2,3-dimethylimidazolium tetrafluoroborate ([Emmim][BF_4]) is synthesized in accordance with

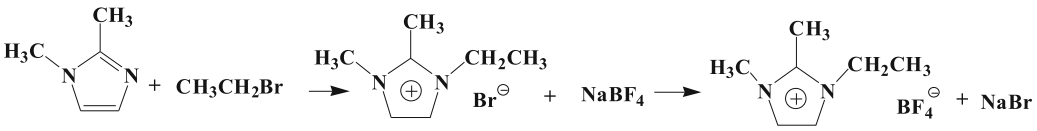

Scheme 1 Synthesis route of IL [Emmim][BF_4]

Table 2 Density, viscosity, and electrical conductivity of binary system [Emmim][BF_4] + ACN at T = (288.15–333.15) K and 101 kPa

c_{IL}	T/K									
	288.15	293.15	298.15	303.15	308.15	313.15	318.15	323.15	328.15	333.15
ρ/g cm^{-3}										
0.2	0.80702	0.80168	0.79648	0.79115	0.78580	0.78043	0.77501	0.76965	0.76435	0.75903
0.4	0.82321	0.81805	0.81284	0.80760	0.80234	0.79707	0.79176	0.78641	0.78107	0.77581
0.6	0.84296	0.83787	0.83273	0.82757	0.82239	0.81720	0.81198	0.80673	0.80163	0.79642
0.8	0.85767	0.85264	0.84755	0.84243	0.83731	0.83223	0.82702	0.82183	0.81678	0.81176
1.0	0.87284	0.86784	0.86281	0.85774	0.85267	0.84759	0.84246	0.83751	0.83254	0.82744
1.2	0.88294	0.87799	0.87299	0.86797	0.86295	0.85792	0.85286	0.84778	0.84297	0.83795
σ/mS cm^{-1}										
0.2	19.9	20.8	21.7	22.6	23.5	24.4	25.3	26.2	27.1	28.0
0.4	32.3	33.5	34.7	35.9	37.2	38.4	39.7	41.1	42.4	43.8
0.6	40.5	42.2	43.9	45.5	47.2	48.9	50.7	52.5	54.3	56.1
0.8	47.5	49.6	51.8	54.1	56.3	58.5	60.8	63.2	65.5	67.7
1.0	52.4	55.0	57.4	59.9	62.5	64.9	67.4	69.8	72.2	74.6
1.2	51.7	54.3	56.9	59.5	62.2	64.8	67.4	69.9	72.7	75.3
η/mPa s										
0.2	0.395	0.376	0.358	0.343	0.328	0.314	0.302	0.291	0.280	0.270
0.4	0.416	0.398	0.379	0.365	0.349	0.336	0.322	0.313	0.302	0.292
0.6	0.435	0.419	0.399	0.384	0.369	0.355	0.343	0.332	0.321	0.311
0.8	0.454	0.438	0.418	0.405	0.388	0.376	0.364	0.353	0.342	0.332
1.0	0.476	0.457	0.439	0.422	0.409	0.394	0.382	0.371	0.361	0.351
1.2	0.496	0.477	0.459	0.444	0.429	0.415	0.403	0.392	0.381	0.371

Standard uncertainties are u (T) = ± 0.01 K, u (P) = ± 10^3 Pa. The relative standard uncertainties are u (ρ) = ± 0.0002 g cm^{-3}, u (σ) = ± 0.1 mS m^{-1}, u (η) = ± 0.003 mPa s

a two-step method (Scheme 1) described with the previous works [26, 27]. The final product is white solid salt. The IL is dried for 48 h under vacuum. The neat IL is then verified by ^{1}H NMR, IR, TGA, and EA. (see supporting information).

Preparation of IL and IL + ACN binary system

A series of [Emmim][BF_4] + ACN binary mixtures are prepared by weighing on a Shanghai JKFA2004N analytical balance with a precision of 0.0001 g. The concentration of

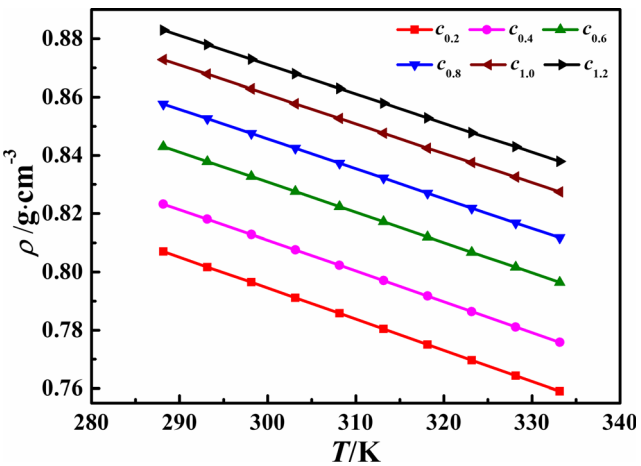

Fig. 1 Density ρ for the [Emmim][BF_4] + ACN binary system as a function of temperature T at different concentrations of the IL

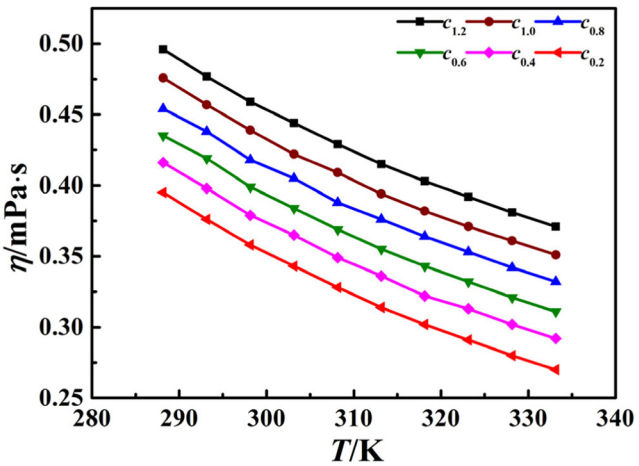

Fig. 2 Viscosity η for the [Emmim][BF_4] + ACN binary system as a function of temperature T at different concentrations of the IL

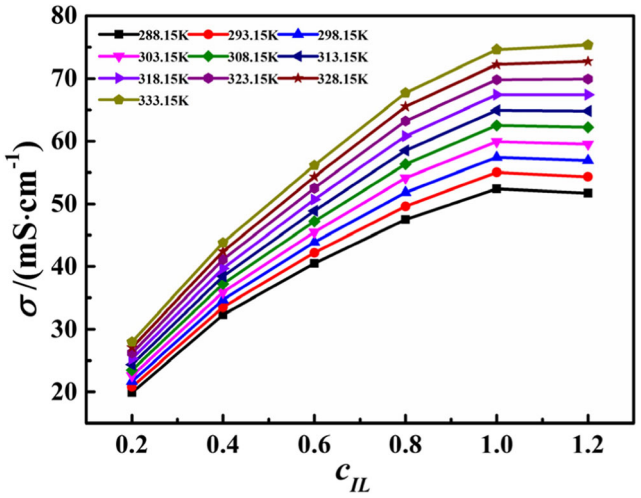

Fig. 3 Electrical conductivities vs concentrations of the IL for the [Emmim][BF_4] + ACN binary system at different temperatures *T*

[Emmim][BF_4] in the mixtures (c_{IL}) are 0.2, 0.4, 0.6, 0.8, 1.0, and 1.2 mol·L^{-1}. These binary mixtures are called $c_{0.2}$, $c_{0.4}$, $c_{0.6}$, $c_{0.8}$, $c_{1.0}$, and $c_{1.2}$, respectively.

Preparation of the supercapacitors

A symmetrical supercapacitor device is designed by two identical electrodes. The electrodes are constituted of the viscous slurry of the active material, carbon black, and 60 wt% polytetrafluoroethylene in a small amount of ethanol mixed in 8:1:1 wt% [28]. The mass of each working electrode is about 80 mg. Each of the working electrodes is 13 mm in diameter and 2 mm in thickness [29–31]. Afterwards, the electrodes were dried at 353.15 K for 36 h.

Measurements

Density

A Mettler Toledo DM45 Delta Range Density Meter was used to measure the densities of the [Emmim][BF_4] + ACN binary mixtures from 288.15 to 333.15 K with a step size of 5 K under atmospheric pressure. Resolution of the apparatus was 0.00001 g cm^{-3}. The uncertainty was ± 0.0002 g cm^{-3} for the density measurement and ± 0.01 K for the temperature. The values are listed in Table 2.

Viscosity

The viscosity of the binary mixtures was measured by an Anton Paar Lovis 2000 M viscometer, using rolling-ball principle. The viscosity range of the standard solution was 10 to 300 mPa s over the temperature range from 288.15 to 333.15 K at 5 K intervals with an accuracy of 0.0001 mPa s under atmospheric pressure. The uncertainty of the viscosity measurement was estimated to be ± 0.003 mPa s. The values are listed in Table 2.

Electrical conductivity

The electrical conductivities of binary mixtures were measured with a DDSJ-308A conductivity meter operating in a DJS-10C conductivity electrode under dry argon atmosphere. Temperature accuracy from 288.15 to 333.15 K was ensured within ± 0.01 K by means of a thermostatic water bath under atmospheric pressure. The uncertainty in the electrical conductivity measurements was estimated to be ± 0.1 mS cm^{-1}. The values are listed in Table 2.

Electrochemical testing

The electrochemical property was measured on coin cells by electrochemical working station. All electrochemical behaviors of the fabricated supercapacitor were tested by cyclic voltammetry (CV), electrical impedance spectroscopy (EIS), and galvanostatic charge-discharge (GCD). The CV and the EIS were measured by an electrochemical working station (CHI 660E), and the GCD was measured by a battery testing system (CT 3008W). The CV curves for supercapacitors were measured at various scan rates (10, 20, 30, 50, 100 mV s^{-1}). The CV curves in different voltage range were measured at the scan rate of 10 mV s^{-1}, and the current densities of GCD were 20 mA g^{-1}. The

Table 3 Fitted parameter values of VFT equation and Arrhenius equation of conductivity for the binary system [Emmim][BF_4] + ACN

c_{IL}	VFT equation				Arrhenius equation		
	D_0/mS cm^{-1}	B/K	T_0/K	R^2	D_∞/mS cm^{-1}	*Ea*/kJ mol^{-1}	R^2
0.2	150.4	445.2	68.31	0.99996	253.8	$6.10 \cdot 10^3$	0.99981
0.4	2791	2743.4	− 327.1	0.99996	305.7	$5.39 \cdot 10^3$	0.99949
0.6	926.0	1218	− 101.2	0.99993	446.2	$5.75 \cdot 10^3$	0.99983
0.8	720.4	812.5	− 10.57	0.99994	662.4	$6.32 \cdot 10^3$	0.99994
1.0	344.2	366.8	93.25	0.99996	716.4	$6.26 \cdot 10^3$	0.99962
1.2	501.2	515.9	61.03	0.99995	834.9	$6.66 \cdot 10^3$	0.99984

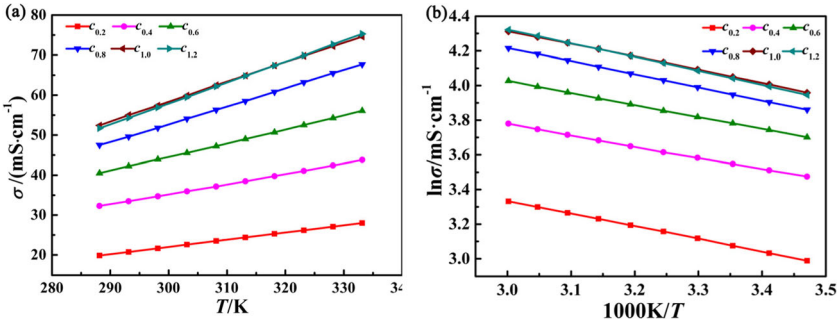

Fig. 4 (**a**) σ vs T and (**b**) lnσ vs T^{-1} for the [Emmim][BF_4] + ACN binary system at different concentrations of the IL.

specific capacitance was calculated from the GCD according to equation the following equations [32]:

$$C = I\Delta t/(m\Delta V) \quad (1)$$

The energy density was figured up from the GCD on the basis of equation:

$$E = {}^{1}/_{2}CV^{2} \quad (2)$$

The power density was computed from the GCD based on equation:

$$P = E/\Delta t \quad (3)$$

where C (F g^{-1}) is capacitance, m (g) is the mass of porous carbon on the working electrode, I (A) is the constant discharging current, Δt (s) is the discharging time, ΔV (V) is the potential window, E (Wh Kg^{-1}) is energy density, and P (KW Kg^{-1}) is power density. The whole electrochemical evaluation was performed at room temperature.

Results and discussion

Density, viscosity, and electrical conductivity

In this study, the density of binary system was measured at temperature from 288.15 to 333.15 K under atmospheric pressure, and the results are listed in Table 2. Figure 1 displays the experimental values of ρ against T. A liner correlation can be found between the density of the binary systems and the temperature, at the range of 288.15 to 333.15 K [33]. The density undulation can be embodied in thermal properties of the electrolyte [34]. From Fig. 1, the density values decreased with the rise of temperature. And at the same temperature, with the increase dosage of ILs, density values increase. The consequence of these binary systems showed a similar trend to the [Bmmim][BF_4] + ACN binary systems in literature [35].

The viscosity and electrical conductivity are usually considered the most important transport properties to evaluate IL for applications involving the use of IL as electrolytes [27]. We examined the viscosity of the binary system with the IL addition from 288.15 to 333.15 K. The relationship between viscosity and temperature is shown in Fig. 2. Like general trend [33], the viscosities of the binary mixtures decrease with the increased temperature. And with the addition of [Emmim][BF_4], both the viscosity and conductivity increase.

The electrical conductivities against concentrations of the IL for the binary mixtures are shown in Fig. 3. As seen from the Fig. 3, a raise of temperature leads to an increase of the electrical conductivity. The electrical conductivity values become larger with the enhanced concentration until the σ_{max} is reached. When $c \approx 1.0$ mol L^{-1}, the values reached the maximum, where conductivity is 55.0 mS cm^{-1} at room temperature. Compared to the similar mixture systems of N-butyl-4-methylpyridinium bis(trifluoromethylsulfonyl)imide ([Bupy][Tf_2N]) + ACN and N-hexylpyridinium bis(trifluoromethylsulfonyl)imide ([Hepy][Tf_2N]) + ACN, whose electrical conductivities

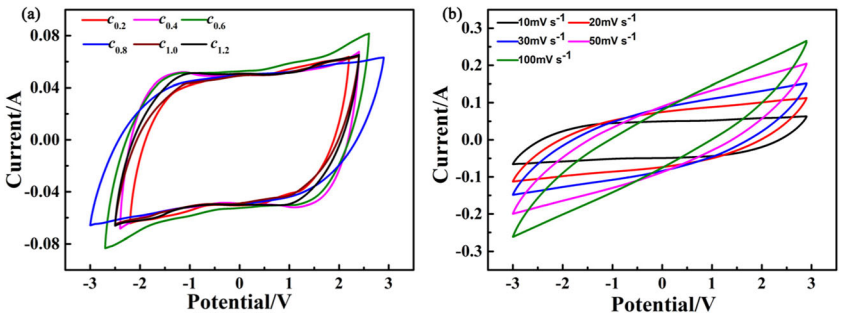

Fig. 5 (**a**) Cyclic voltammograms for the [Emmim][BF_4] + ACN binary system at different concentrations of the IL. The voltage scan rate is 10 mV s^{-1} (**b**) CV curves for the $c_{0.8}$ at scan rates range from 1 m to 100 mV s^{-1}

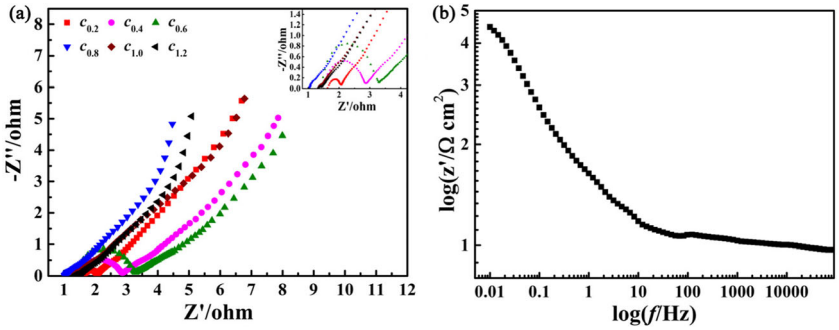

Fig. 6 (**a**) Nyquist plots for the [Emmim][BF_4] + ACN binary system at different concentrations of the IL. (**b**) Dependencies of log Z' vs. log f plots for binary system in $c_{0.8}$

are 40.12 and 33.99 mS cm^{-1} [36], the electrical conductivities are smaller than the binary system in this work.

Then, the relation of temperature and electrical conductivity of IL [Emmim][BF_4] + ACN can be fitted by the Vogel-Fulcher-Tamman (VFT) equation [26] as the following, respectively:

$$D = D_0 \exp\left[-B/(T-T_0)\right] \quad (4)$$

where D is conductivity, D_0 is the conductivity at the temperature limit, B is the quantity related to the activation barrier, and T_0 is the absolute or "ideal glass transition" temperature. The fitted VFT parameters are listed in Table 3.

For electrical conductivity, the Arrhenius equation is:

$$D = D_\infty \exp[-E_a/(RT)] \quad (5)$$

where E_a is the activation energy for conductivity, which showed the energy needed for an ion to hop to a free hole, D_∞ is the maximum conductivity, and R is the gas constant. According to the Arrhenius equation, the $1/T$ relied on $\ln\sigma$ is plotted. (see Fig. 4b). The correlation coefficients of the VFT equation were all > 0.99993, and correlation coefficients of Arrhenius equation were nearly 0.999, which shows that the VFT equation should be proper for describing the effect of temperature on the conductivity of IL.

Electrochemical testing

The electrochemical stability of the binary mixtures is investigated by cyclic voltammetry (CV). Figure 5a presents the CV curves of the fabricated supercapacitors using the mixture electrolytes with various [Emmim][BF_4] concentrations at scan rate of 10 mV s^{-1} under the room temperature. All the CV curves maintain well rectangular shape, which indicate a typical double layer behavior with the electrolyte ions unimpeded diffusion within the practicable electrode surface [37]. As the concentration of [Emmim][BF_4] in binary electrolytes increase from 0.2 to 0.8 mol·L^{-1}, the potential window enhanced to the maximum value(5.9 V). This result may be related to its high conductivity and medium viscosity. The CV curves of the $c_{0.8}$ at different scan rates from 10 to 100 mV s^{-1} are presented in Fig. 5b. The rectangular shape of CV curves at low scan rates indicates that the mobile charge carriers diffuse at an almost constant rate and form the ion accumulation with low ohmic resistance [38]. The CV curves show slightly deviations at high scan rate because of electrode polarization effects and reduced electrolyte mobility in small pore regions [39].

Figure 6a displays the Nyquist plots of the mixture electrolytes at room temperature. As seen from the figure, the Nyquist plots exhibit typical double-layer capacitor characteristics. In the high-frequency region, the series resistance (Rs) of the supercapacitor is the intercept on the X-axis. It is caused by electrolyte solution resistance, separator paper, and external circuit resistance. The semi-circle represents the contact resistance (Rct) between the electrode and the electrolyte. In the low frequency range, the straight line represents capacitance characteristics [40–42]. The 45° sloped curve is the Warburg resistance, and it is a result of the frequency dependence on ion diffusion/transport in the electrolyte to the

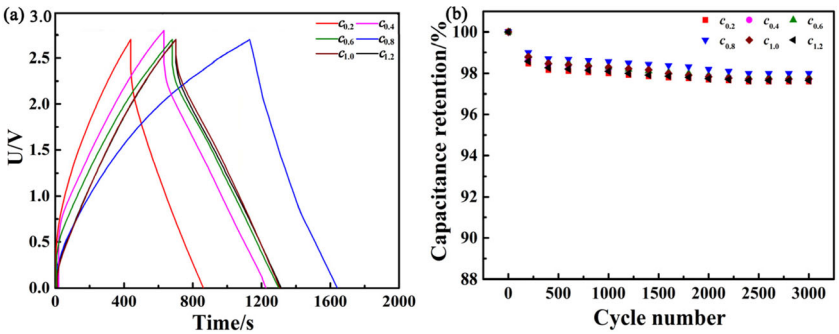

Fig. 7 (**a**) Galvanostatic charge-discharge curve for the [Emmim][BF_4] + ACN binary system at different concentrations of the IL under a constant current density of 20 mA g^{-1}. (**b**) Cycle performance for the supercapacitor after 3000 cycles of charging and discharging at a current density of 20 mA g^{-1}

Table 4 Capacitance, energy, density and power density of binary system [Emmim][BF_4] + ACN

c_{IL} (mol L^{-1})	C (F g^{-1})	E (Wh Kg^{-1})	P (KW Kg^{-1})
0.2	86.41	21.87	2.68
0.4	104.5	26.37	2.67
0.6	117.7	29.78	2.69
0.8	142.6	36.10	2.75
1.0	137.0	34.69	2.78
1.2	131.9	33.38	3.00

electrode surface. As is shown in Fig. 6, the electrolyte solution resistance decreases with increasing concentration of [Emmim][BF_4] ionic liquid. When the ionic liquid concentration reaches $c_{0.8}$, the internal resistance of the electrolyte solution is the minimum. The high transferability and solubility can help ions insert into the hole of activated carbon. These reduce the interfacial resistance between electrode and electrolyte availably [41].

Figure 6b shows that the high frequency series resistance is independent of potential applied, and therefore, the electrolyte series resistance R_s can be calculated at $f \geq 10$ kHz. At low frequencies, the values of log Z' increased, which is adsorption and diffusion limited stages in the interior of the electrolyte [43]. The result is caused mainly by the surface roughness of the electrode [44–46].

The galvanostatic charge-discharge profiles of mixture electrolytes with different IL concentrations (Fig. 7a) were recorded with two-electrode supercapacitor at the current density of 20 mA g^{-1} in the voltage from 0.0 to 2.7 V. All the curves are linear and symmetrical triangle, indicating the excellent electrochemical reversibility and typical charge-discharge features of double layer capacitor [47]. The galvanostatic charging-discharging duration time for supercapacitor varied with the IL concentrations of the mixture electrolytes, which is in good agreement with the CVs and the impedance plots (Figs. 5 and 6). The charge/discharge performance of supercapacitor using $c_{0.8}$ electrolyte with the longest duration times and without visible sudden voltage drop (IR drop) is obviously superior to those of other five systems electrolytes. After 3000 cycles at the working voltage of 2.7 V, capacitance retentions of EDLCs using $c_{0.8}$ electrolyte (Fig. 7b) is reduced to 98%.

The electrochemical performance is also analyzed. The capacitance (C, F g^{-1}), energy density (E, Wh Kg^{-1}), and power density (P, kW kg^{-1}) were calculated according to the Eqs. (1)–(3), and the results are listed in Table 4. After a short period of stabilization, the specific capacitance can achieve 142.6 F g^{-1}, and the maximum storage energy is calculated to be 36.1 Wh Kg^{-1} at a current density of 20 m Ag^{-1}. Compare with [Pyr_{14}][TFSI] + ACN, [Pyrr][NO_3] + gamma butyrolactone (γ-BL), the specific capacitance values of [PYR_{14}][TFSI] + ACN, [Pyrr][NO_3] + γ-BL are about 31,125 F g^{-1},which are smaller than our binary system [48, 49].

Conclusion

In this paper, an IL-based binary mixture system of [Emmim][BF_4] + ACN was prepared, and the physicochemical properties and the electrochemical performances in supercapacitors of the system were studied. The different concentrations of [Emmim][BF_4] in the mixture electrolyte can provide different voltage windows and capacitances. The electrical conductivity of the mixture of 1.0 mol L^{-1} can reach 55.0 mS cm^{-1} at the room temperature. The voltage window of the symmetrical AC supercapacitor with the IL mixture electrolyte could be expanded up on 5.9 V ($c_{IL} \approx 0.8$). The high solubility, low viscosity, and good conductivity of the ionic liquid can explain the capacity of the electrolyte in electrochemical applications. Due to introducing the ionic liquids into the ACN, the density, viscosity, and electrical conductivity of the mixture electrolyte were increased. And the specific capacitance, power density, and energy density of the fabricated supercapacitors using the mixture electrolyte are also improved.

Funding information This work was financially supported by the National Nature Science Foundation of China (no. 21503020, no. 21373002). The Nature Science Foundation of Liaoning Province (no. 201602016). The Doctoral Fund of Liaoning Province of China (no. 201601347). Program for Liaoning Excellent Talents in University, China (LJQ2015099). Project of Education Department of Liaoning Province of China (no. LQ2017014).

References

1. Simon P, Gogotsi Y (2008) Materials for electrochemical capacitors. Nat Mater 7:845–854
2. Pandolfo AG, Hollenkamp AF (2006) Carbon properties and their role in supercapacitors. J Power Sources 157:11–27
3. Hashmi SA, Updahyaya HM (2002) MnO_2-polypyrrole conducting polymer composite electrodes for electrochemical redox supercapacitors. Ionics 8:272–277
4. Liu S, Dong HF, Du JP, Qin XJ, Shao GJ (2014) MnO_2/graphite electrodeposited under supergravity field for supercapacitors and its electrochemical properties. Ionics 20:295–299
5. Huang GY, Zhang WJ, Xu SM, Li YJ, Yang Y (2016) Microspherical ZnO synthesized from a metal-organic precursor for supercapacitors. Ionics 22:2169–2174
6. Portet C, Yushin G, Gogotsi Y (2008) Effect of carbon particle size on electrochemical performance of EDLC. J Electrochem Soc 155: A531–A536
7. Xu B, Wu F, Chen R, Cao G, Chen S, Zhou Z, Yang Y (2008) Highly mesoporous and high surface area carbon: a high capacitance electrode material for EDLCs with various electrolytes. Electrochem Commun 10:795–797
8. Frackowiak E, Lota G, Machnikowski J, Vix-Guterl C, Beguin F (2006) Optimisation of supercapacitors using carbons with controlled nanotexture and nitrogen content. Electrochim Acta 51: 2209–2214

9. Conway BE (1999) Electrochemical capacitors. Kluwer Academic Plenum Publisher, New York
10. Portet C, Taberna PL, Simon P, Laberty-Robert C (2004) Modification of Al current collector surface by sol–gel deposit for carbon–carbon supercapacitor applications. Electrochim Acta 49: 905–912
11. Perricone E, Chamas M, Leprêtre JC, Judeinstein P, Azais P, Raymundo-Pinero E, Béguin F, Alloin F (2013) Safe and performant electrolytes for supercapacitor. Investigation of esters/carbonate mixtures. J Power Sources 239:217–224
12. Lei C, Amini N, Markoulidis F, Wilson P, Tennison S, Lekakou C (2013) Activated carbon from phenolic resin with controlled mesoporosity for an electric double-layer capacitor (EDLC). J Mater Chem A 1:6037–6042
13. Weingarth D, Noh H, Foelske-Schmitz A, Wokaun R, Kötz A (2013) A reliable determination method of stability limits for electrochemical double layer capacitors. Electrochim Acta 103:119–124
14. Zhang LL, Zhao XS (2009) Carbon-based materials as supercapacitor electrodes. Chem Soc Rev 38:2520–2531
15. Denshchikov KK, Izmaylova MY, Zhuk AZ, Vygodskii YS, Novikov VT, Gerasimov AF (2010) 1-Methyl-3-butylimidazolium tetraflouroborate with activated carbon for electrochemical double layer supercapacitors. Electrochim Acta 55: 7506–7510
16. Arbizzani C, Biso M, Cericola D, Lazzari M, Soavi F, Mastragostino M (2008) Safe, high-energy supercapacitors based on solvent-free ionic liquid electrolytes. J Power Sources 185: 1575–1579
17. Béguin F, Presser V, Balducci A, Frackowiak E (2014) Supercapacitors: carbons and electrolytes for advanced supercapacitors (Adv. Mater. 14/2014). Adv Mater 26:2283–2283
18. Galiński M, Lewandowski A, Stępniak I (2006) Ionic liquids as electrolytes. Electrochim Acta 51:5567–5580
19. Lazzari M, Mastragostino M, Soavi F (2007) Capacitance response of carbons in solvent-free ionic liquid electrolytes. Electrochem Commun 9:1567–1572
20. Lazzari M, Soavi F, Mastragostino M (2008) High voltage, asymmetric EDLCs based on xerogel carbon and hydrophobic IL electrolytes. J Power Sources 178:490–496
21. Mastragostino M, Soavi F (2007) Strategies for high-performance supercapacitors for HEV. J Power Sources 174:89–93
22. Tanahashi I, Yoshida A, Nishino A (1990) Electrochemical characterization of activated carbon-fiber cloth polarizable electrodes for electric double-layer capacitors. J Electrochem Soc 137:3052–3057
23. Brandt A, Ramirez-Castro C, Anouti M, Balducci A (2013) An investigation about the use of mixtures of sulfonium-based ionic liquids and propylene carbonate as electrolytes for supercapacitors. J Mater Chem A 1:12669–12678
24. Schütter C, Neale AR, Wilde P, Goodrich P, Hardacre C, Passerini S, Jacquemin J, Balducci A (2016) The use of binary mixtures of 1-butyl-1-methylpyrrolidinium bis {(trifluoromethyl) sulfonyl} imide and aliphatic nitrile solvents as electrolyte for supercapacitors. Electrochim Acta 220:146–155
25. Huang PL, Luo XF, Peng YY, Pu NW, Ger MD, Yang CH, Wu TY, Chang JK (2015) Ionic liquid electrolytes with various constituent ions for grapheme based supercapacitors. Electrochim Acta 161: 371–377
26. Zhang QG, Li MC, Zhang XY, Wu XY (2014) The thermodynamic estimation and viscosity, electrical conductivity characteristics of 1-alkyl-3-methylimidazolium thiocyanate ionic liquids. Z Phys Chem 228:851–867
27. Zhang QG, Lan YL, Liu HW, Zhang XY, Zhang XL, Wei Y (2016) Estimation and structural effect on physicochemical properties of alkylimidazolium-based ionic liquids with different anions. J Chem Eng Data 61:2002–2012
28. Liu CY, Ma XD, Xu F, Zheng LP, Zhang H, Feng WF, Huang XJ, Armand M, Nie J, Chen HL, Zhou ZB (2014) Ionic liquid electrolyte of lithium bis(fluorosulfonyl)imide/N-methy-N-propylpiperidiniumbis (fluorosulfonyl)imide for Li/natural graphite cells: effect of concentration of lithium salt on the physicochemical and electrochemical properties. Electrochim Acta 149:370–385
29. Wang B, Al Abdulla W, Wang D, Zhao XS (2015) A three-dimensional porous $LiFePO_4$ cathode material modified with a nitrogen-doped graphene aerogel for high-power lithium ion batteries. Energy Environ Sci 8:869–875
30. Wang B, Xie Y, Liu T, Luo H, Wang B, Wang CH, Wang L, Wang DL, Dou SX, Zhou Y (2017) $LiFePO_4$ quantum-dots composite synthesized by a general microreactor strategy for ultra-high-rate lithium ion batteries. Nano Energy 42:363–372
31. Wang B, Liu T, Liu A, Liu GJ, Wang L, Gao TT, Wang DL, Zhao XS (2016) A hierarchical porous C@ $LiFePO_4$/carbon nanotubes microsphere composite for high-rate lithium-ion batteries: combined experimental and theoretical study. Adv Energy Mater 6:1-10(1600426). https://doi.org/10.1002/aenm.201600426
32. Stoller MD, Ruoff RS (2010) Best practice methods for determining an electrode material's performance for ultracapacitors. Energy Environ Sci 3:1294–1301
33. Wei Y, Wang B, Zhao Z, Zhang XY, Wu XY, Zhang QG (2015) Estimation of physico-chemical properties and structure characteristics of new alkylimidazolium salicylate ionic liquids. Z Phys Chem 230:1165–1183
34. Rocha MAA, Coutinho JAP, Santos LMNBF (2013) Evidence of nanostructuration from the heat capacities of the 1,3-dialkylimidazolium bis(Trifluoromethylsulfonyl)imide ionic liquid series. J Chem Phys 139:104502
35. Ciocirlan O, Iulian O (2012) Properties of pure 1-butyl-2,3-dimethylimidazolium tetrafluoroborate ionic liquid and its binary mixtures with dimethyl sulfoxide and acetonitrile. J Chem Eng Data 57:3142–3148
36. Zhang QG, Sun SS, Pitula S, Liu QS, Welz-Biermann U, Zhang GG (2011) Electrical conductivity of solutions of ionic liquids with methanol, ethanol, acetonitrile, and propylene carbonate. J Chem Eng Data 56:4659–4664
37. Inagaki M, Konno H, Tanaike O (2010) Carbon materials for electrochemical capacitors. J Power Sources 195:7880–7903
38. Arof AK, Kufian MZ, Syukur MF, Aziz MF, Abdelrahman AE, Majid SR (2012) Electrical double layer capacitor using poly(methyl methacrylate)-C_4BO_8Li gel polymerelectrolyte and carbonaceous material from shells of mata kucing (Dimocarpus longan) fruit. Electrochim Acta 74:39–45
39. DeRosa D, Higashiya S, Schulz A, Fondacaro MR, Haldar P (2017) High performance spiro ammonium electrolyte for electric double layer capacitor. J Power Sources 360:41–47
40. Kang J, Wen J, Jayaram SH, Yu A, Wang X (2014) Development of an equivalent circuit model for electrochemical double layer capacitors (EDLCs) with distinct electrolytes. Electrochim Acta 115: 587–598
41. Liu W, Yan X, Lang J, Xue Q (2011) Electrochemical behavior of graphene nanosheets in alkylimidazolium tetrafluoroborate ionic liquid electrolytes: influences of organic solvents and the alkyl chains. J Mater Chem 21:13205–13212
42. Tõnurist K, Thomberg T, Jänes A, Romann T, Sammelselg V, Lust E (2013) Influence of separator properties on electrochemical performance of electrical double-layer capacitors. J Electroanal Chem 689:8–20
43. Härk E, Nerut J, Vaarmets K, Tallo I, Kurig H, Eskusson J, Kontturi K, Lust E (2013) Electrochemical impedance characteristics and electroreduction of oxygen at tungsten carbide derived micromesoporous carbon electrodes. J Electroanal Chem 689: 176–184

44. Lust E, Jänes A, Sammelselg V, Miidla P, Lust K (1998) Surface roughness of bismuth, antimony and cadmium electrodes. Electrochim Acta 43:373–383
45. Lust E, Jänes A, Sammelselg V, Miidla P (2000) Influence of charge density and electrolyte concentration on the electrical double layer characteristics at rough cadmium electrodes. Electrochim Acta 46:185–191
46. Lust E, Jänes A, Lust K, Sammelselg V, Miidla P (1997) Influence of surface pretreatment of bismuth and cadmium electrodes to the electric double layer and adsorption characteristics of organic compounds. Electrochim Acta 42:2861–2879
47. Cheng F, Yu X, Wang J, Shi ZQ, W C C (2016) A novel supercapacitor electrolyte of spiro-(1, 1′)-bipyrolidinium tetrafluoroborate in acetonitrile/dibutyl carbonate mixed solvents for ultra-low temperature applications. Electrochim Acta 200:106–114
48. Anouti M, Timperman L (2013) A pyrrolidinium nitrate protic ionic liquid-based electrolyte for very low-temperature electrical double-layer capacitors. Phys Chem Chem Phys 15:6539–6548
49. Vaquero S, Palma J, Anderson M, Marcilla R (2013) Improving performance of electric double layer capacitors with a mixture of ionic liquid and acetonitrile as the electrolyte by using mass-balancing carbon electrodes. J Electrochem Soc 160:A2064–A2069